β-delayed proton emission from ^{26}P and ^{27}S

Ł. Janiak,[1] N. Sokołowska,[1,2] A. A. Bezbakh,[3] A. A. Ciemny,[1] H. Czyrkowski,[1] R. Dąbrowski,[1] W. Dominik,[1]
A. S. Fomichev,[3] M. S. Golovkov,[3,4] A. V. Gorshkov,[3] Z. Janas,[1] G. Kamiński,[3,5] A. G. Knyazev,[3,6] S. A. Krupko,[3] M. Kuich,[1]
C. Mazzocchi,[1] M. Mentel,[2,3] M. Pfützner,[1] P. Pluciński,[2,3] M. Pomorski,[1] R. S. Slepniev,[3] and B. Zalewski[3,7]

[1]*Faculty of Physics, University of Warsaw, 02-093 Warszawa, Poland*
[2]*AGH University of Science and Technology, Faculty of Physics and Applied Computer Science, 30-059 Kraków, Poland*
[3]*Joint Institute for Nuclear Research, 141980 Dubna, Moscow Region, Russia*
[4]*Dubna State University, Dubna, Russia*
[5]*Institute of Nuclear Physics PAN, 31-342 Kraków, Poland*
[6]*Department of Physics, Lund University, SE-22100 Lund, Sweden*
[7]*Heavy Ion Laboratory, University of Warsaw, 02-093 Warszawa, Poland*

Delayed emission of protons following β decay of neutron deficient nuclei ^{26}P and ^{27}S was investigated at the ACCULINNA separator in the Flerov Laboratory of Nuclear Reactions at Dubna. Ions of interest, identified in flight, were implanted into the active volume of the gaseous optical time projection chamber, which allowed us to record tracks of charged particles emitted in the decay. Total branching ratios for β-delayed proton emission and for β-delayed two-proton emission were determined. In addition, energy spectra for delayed protons below 2 MeV were established. Our findings for ^{26}P agree with results of previous experiments. In the case of ^{27}S, however, the observed probability of delayed proton emission is an order of magnitude larger than reported in literature. Two new strong proton transitions were identified representing decays of the first two excited states of ^{27}P to the ground state of ^{26}Si. The probability ratio of γ-to-proton emission from these states is discussed.

I. INTRODUCTION

Experimental techniques and instrumentation developed in recent decades allow us to access the most neutron-deficient nuclei, up to the proton drip line and beyond, for almost all elements below bismuth [1,2]. Nevertheless, in spite of substantial efforts to investigate these nuclei, our knowledge of their properties and our understanding of their structure is far from complete. Yet this knowledge is important to learn if and how a large neutron deficiency alters nuclear structure, to test fundamental symmetries, and to provide input data for modeling astrophysical phenomena, such as the rp process.

A very important tool in studies of unstable nuclei is β decay, which offers insight into the structure of the initial and the final states. For very neutron-deficient nuclei, β decay has a feature of special importance. Due to the large decay energy, Q_{EC}, unbound states in the daughter nuclei can be populated, followed by emission of β-delayed charged particles. Since detection of such particles is easier and more efficient than detection of γ rays, they represent a valuable source of information, particularly for the most exotic nuclei which are usually produced in small quantities. On the other hand, the complete knowledge of the decay scheme, including all particle emission channels, is required for the correct determination of the β strength, which bears structural information. Some delayed particle emission channels have an additional advantage when they represent a reverse process to the radiative capture reaction of astrophysical significance. For example, β-delayed proton emission (βp) can be used to characterize a resonance playing a key role in a ($p,γ$) reaction. This is especially worthwhile when the study of the direct reaction is hampered by the low intensity of the radioactive beam.

In this context, decay study of ^{26}P and of ^{27}S is of interest. Both decays contribute to the complete understanding of the nucleosynthesis of ^{26}Al, which is a cosmic γ-ray emitter observed in the interstellar medium by satellite-based γ telescopes [3]. In high-temperature environments, like in novae explosions, ^{26}Al is produced by the reaction chain [4]: ^{24}Mg($p,γ$)^{25}Al($β^+,ν$)^{25}Mg($p,γ$)^{26}Al. However, this sequence can be bypassed by the proton capture reactions ^{25}Al($p,γ$)^{26}Si($p,γ$)^{27}P [4]. One way to constrain the rates of these reactions is by the study of β decay of ^{26}P and ^{27}S, respectively, followed by delayed emission of protons and γ rays.

A great deal is already known about these two cases. The β decay of ^{26}P was studied by Thomas *et al.* by means of charged-particle and γ-ray spectroscopy [5]. The half-life of ^{26}P was determined to be $T_{1/2} = 43.7(6)$ ms. A very rich spectrum of βp was established. The strongest proton line, at the energy of 412(2) keV and with an absolute intensity of 18%, was found to represent a transition from the 3_3^+ state at 5.93 MeV in ^{26}Si to the ground state of ^{25}Al. This transition is relevant to the production of ^{26}Al mentioned above. The total branching for the delayed proton emission from ^{26}P was found to be 39(2)%. This value includes the 2.2% contribution from the β-delayed two-proton emission (β$2p$). Two lines were assigned to this decay channel, based on energy considerations, as only the total decay energy was measured in a stack of silicon detectors. More recently, the detailed γ spectroscopy of ^{26}P was performed with a high efficiency array of germanium detectors [6]. The main finding was the observation of a γ transition depopulating the 3_3^+ state in ^{26}Si which allowed constraint of ^{26}Al production in classical novae events. Among other results, the energy of the proton transition

from this state was determined with better accuracy and was found to be $414.9 \pm 0.6(\text{stat}) \pm 0.3(\text{syst}) \pm 0.6(\text{lit})$ keV [6]. In addition, the complete data analysis of this experiment revealed β-decay asymmetry between ^{26}P and its mirror ^{26}Na, which was interpreted as possible evidence for the proton halo in ^{26}P [7].

Charged particles and γ rays following β decay of ^{27}S were measured by Canchel *et al.* [8] using a silicon-detector telescope and a germanium detector. The half-life of ^{27}S was measured to be $T_{1/2} = 15.5(15)$ ms. Three lines in the energy spectrum of delayed particles were assigned to βp emission and two lines were interpreted as $\beta 2p$ transitions between the isobaric analog state (IAS) in ^{27}P and the ground state and an excited state in ^{25}Al. The total branching ratio for emission of protons after β decay of ^{27}S was measured to be 5.3(18)%. In this number 1.1(5)% represents $\beta 2p$ emission. As in the case of ^{26}P, the identification of $\beta 2p$ channels was based only on energy considerations. The spectrum of delayed particles was measured only for the energy above 2000 keV. No low-energy proton lines were observed. To constrain the rate of the ^{26}Si$(p,\gamma)^{27}$P reaction states in ^{27}P were investigated using the (^{7}Li , ^{8}He) reaction on a ^{28}Si target [9], by Coulomb dissociation of a ^{27}P beam at 54 MeV/nucleon on a lead target [10], and at 500 MeV/nucleon on a carbon target [11]. The first excited state in ^{27}P, with spin and parity $3/2^+$ [12], which is the dominant resonance for the radiative proton capture by ^{26}Si, was identified. For its excitation energy, determined by particle spectroscopy and kinematical reconstruction, the values 1199(19) keV [9], 1176(32) keV [10], and 1137(33) keV [11] were obtained. The second excited state ($5/2^+$ [12]) was also observed at the energy 1631(19) keV [9], 1666(42) keV [10], and 1592(62) keV [11]. The most precise energy for the $3/2^+$ state in ^{27}P was measured in an experiment combining one-proton knockout reaction from a beam of ^{28}S and γ spectroscopy [13]. A clear γ line in the Doppler-corrected spectrum yielded the value of 1120(8) keV [13].

In this paper we present results of β decay study of ^{26}P and ^{27}S focused on emission of delayed protons. Experiments using silicon detectors (as in Refs. [5,8]) suffer from background due to β particles which is particularly disadvantageous in the low-energy part of the spectrum. We follow a different approach by implanting ions of interest into a gaseous time projection chamber (TPC) which records tracks of charged particles emitted in the decay while being almost insensitive to β electrons. A detector of this type, which combines the TPC concept with optical readout of signals, was developed at the University of Warsaw [14]. This optical time projection chamber (OTPC) was particularly successful in studies of decays with multiparticle emission, such as two-proton radioactivity [15,16] and β-delayed emission of two and three protons [17–19]. The main advantages of the OTPC are the almost complete lack of background and clear identification of decay channels with emission of charged particles. This feature makes it ideal for the determination of branching ratios for such channels. We applied the OTPC to record protons emitted after β decay of ^{26}P and ^{27}S. This allowed us to measure the total branching ratios for βp and $\beta 2p$ decays. In addition, the low-energy part of βp spectrum

was obtained for these two cases. For ^{26}P we found a good agreement with literature. In the case of ^{27}S, however, we observed strong βp channels at low energy, never seen before.

II. EXPERIMENTAL TECHNIQUE

The experiment was carried out at the Flerov Laboratory of Nuclear Reactions in the Joint Institute for Nuclear Research, Dubna, Russia. The ions of interest were produced in a fragmentation reaction by bombarding a 300 μm thick beryllium target with a ^{32}S beam with an energy of 51.3 MeV/nucleon. Then they were separated from contaminants using the AC-CULINNA fragment separator [20] in the achromatic setting with a beryllium degrader, 300 μm thick, mounted at the intermediate focal plane. Selected ions were transferred to the experimental vault downstream of the final focus, where the OTPC detector system was mounted. The setting of the separator was tuned for the optimal transmission of ^{27}S.

Each fragment arriving at the detector was identified using the time-of-flight and energy-loss technique. The time of flight (TOF) was measured between a plastic scintillator, positioned at the middle focal plane of the separator, and a second plastic detector placed at the final focal plane. The energy loss (ΔE) was measured by a Si detector. The average rate of all ions arriving at the final focus was about 3000 ions/s. The rate of ^{27}S was, on average, about 30 ions per hour. A variable aluminum degrader, in front of the OTPC entrance window, was used to tune the implantation depth of ions in the active gas volume.

The OTPC detector is described in more detail in Ref. [16]. Here we present only the main features and some details specific to the reported experiment. The detector volume was filled with a gas mixture of 49.5% Ar, 49.5% He, and 1% CO_2 at atmospheric pressure. The length of the active volume along the beam direction was 35 cm. A uniform, vertical electric field of 130 V/cm, perpendicular to the beam axis, was maintained inside the chamber. Primary electrons, resulting from the gas ionization by the stopping ion and by the emitted charged particles, drifted with constant velocity toward the amplification section, passing through a gating electrode. By changing the potential of this electrode, we could either block most of the primary ionization electrons (low sensitivity to record ions) or let them pass to the amplification section (high sensitivity for decay products). To amplify the signal a stack of four gas electron multiplier (GEM) foils [21] was used, followed by a wire mesh anode. At the anode plane electrons stimulated atoms in the gas to emit light. This light was recorded by a digital camera (CCD) and a photomultiplier (PMT) connected to an oscilloscope. The CCD image provided a projection of particle tracks on the plane of the anode, integrated over an exposure time of 50 ms. The PMT waveform represented the total light intensity as a function of time, which allowed for a determination of the time between the implantation and the decay. In addition, the PMT signal contained information on the projection of the particle tracks along the direction of the electric field, i.e., perpendicular to the anode plane. With known drift velocity, the combination of data from the CCD and the PMT can be used to reconstruct the track of a particle in three dimensions.

The OTPC acquisition system was triggered selectively, based on the TOF information for the incoming ion. The trigger signal was activated only by ions for which the TOF value was below a certain limit. This limit was adjusted to accept all ions of ^{27}S. In addition, some of the ^{26}P and ^{24}Si ions were accepted as well. The trigger signal was used also to flip the sensitivity of the OTPC from low to high, and to switch the beam off to prevent other ions from entering the detector while waiting for the decay of the ion which triggered the system. For each event the identifying (ID) information for the triggering ion was recorded. The ΔE signal from the Si detector, pre-amplified and processed by a fast amplifier, as well as the signal from the time-to-amplitude converter (TAC) representing the TOF of the ion, were fed to the oscilloscope which recorded its full waveform. After the CCD exposure was finished, all event data, including the CCD image, the waveform of the PMT signal, and the waveform of the ID signals, were read and stored on a disk.

The counting gas flowing out of the OTPC chamber was passing through a small chamber designed to measure the electron drift velocity. This was realized by recording the time of passage of ionization electrons, induced by α particles from a radioactive source, over a known distance. Throughout the experiment, the drift velocity, the atmospheric pressure and the temperature were constantly monitored. The two latter parameters were used to calculate the gas density. The average drift velocity was 0.95 cm/μs.

III. DATA ANALYSIS AND RESULTS

From the ID information of each recorded event, the identification spectrum of all ions which triggered the OTPC system was constructed. This spectrum is presented in Fig. 1 together with gates used to select events corresponding to the ions of interest. We identified 2497 events of ^{26}P and 1267 events of ^{27}S. For each of these events we inspected
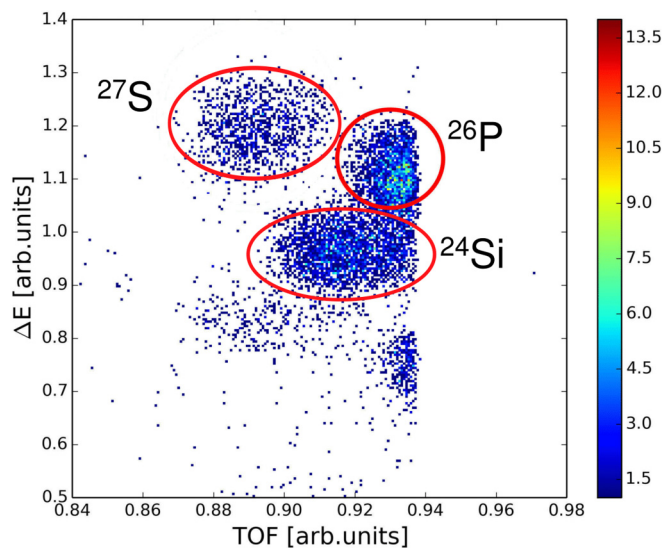

FIG. 1. The identification spectrum showing all ions which triggered the OTPC acquisition system. The identified nuclei of interest are indicated.
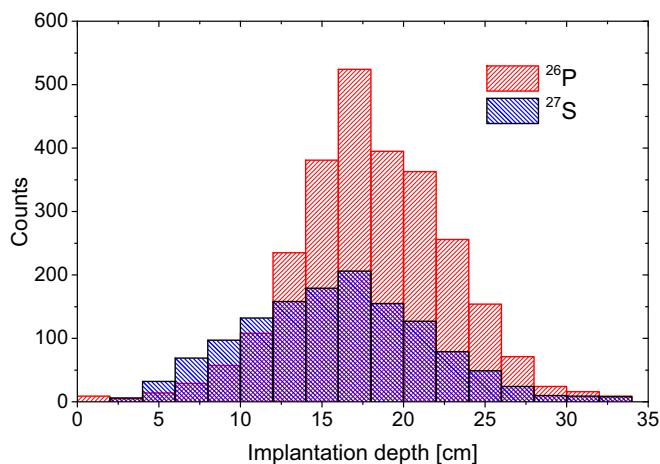

FIG. 2. The range distribution of ^{26}P and ^{27}S ions in the OTPC gas volume.

the corresponding CCD image to determine the implantation depth of the ion in the OTPC detector. The resulting range distributions for both nuclei are shown in Fig. 2. As can be seen, most of the ions were stopped close to the center of the active volume. For further analysis we took only those ions which were stopped at least 2 cm away from the front and the end wall of the detector. This restriction was made to ensure that proton(s) emitted in the decay of the stopped ion will not escape through the wall unnoticed. For directions perpendicular to the beam axis such a correction was not necessary, because the transversal spread of incoming ions was smaller than the 8×3 cm^2 entrance window of the detector, which was located at the center of the 20×21 cm^2 front wall. Finally, the number of identified and well implanted ions was 2463 and 1237 for ^{26}P and ^{27}S, respectively. In the identification plot, shown in Fig. 1 many events corresponding to ^{24}Si are seen as well. We found, however, that a large majority of these ions passed through the active volume of the detector and were stopped beyond it. Therefore, decay of this nuclide could not be analyzed.

From the CCD image of each event one can see whether β-delayed protons were emitted in the decay of the stopped ion during the exposure time. Usually it can be clearly seen how many protons were emitted, even if they escaped the active detector volume. Hence, total branching ratios for different emission channels can be determined by counting and correcting for the limited observation time. If in addition an emitted proton is stopped within the detector volume, its energy and emission direction can be reconstructed from the CCD and the PMT data. To determine the branching ratio as a function of energy, it is important to know what is the probability that the track of a proton of a given energy will be fully contained within the detector volume. We estimated this probability using Monte Carlo simulations. The range of protons in the detector gas was calculated with the SRIM code [22]. Taking into account the observed distribution of the stopped ions (Fig. 2), the detector geometry, and assuming isotropic emission of protons, we obtained the efficiency curves shown in Fig. 3. The small difference between curves
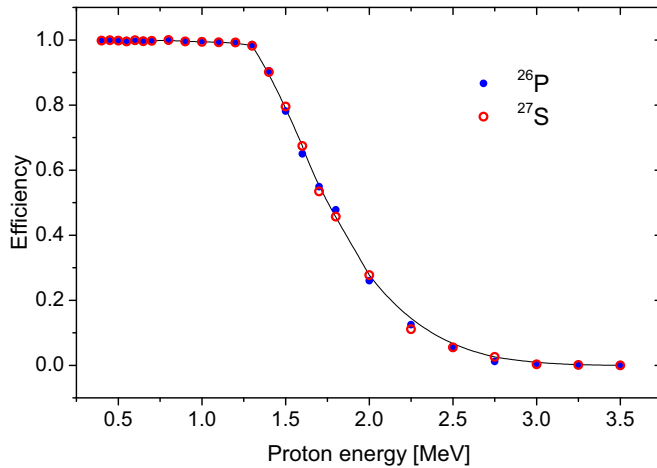
FIG. 3. The calculated probability that the β-delayed proton emitted from ^{26}P and ^{27}S will stop within the active volume of the OTPC detector as the function of the proton energy. The solid line is plotted to guide the eye.

for ^{26}P and ^{27}S results from the difference in the range distribution of these ions. It can be seen that the probability of stopping a proton within the active detector volume is almost 100%, up to a proton energy of 1.3 MeV for both ions of interest.

For those delayed protons which were stopped within the detector, the energy reconstruction was attempted. It was done essentially by comparison of the observed length of the proton track with the SRIM code simulation. For a given gas mixture and its density, the SRIM code yields the relation between the proton energy and the length of its track in the gas, as well as the energy-loss profile along the track. The horizontal and vertical components of the track were derived from the CCD image and the PMT waveform, respectively. First, the length of the horizontal projection was read directly from the image. Then, the shape of the PMT waveform, representing the vertical component, was fitted with the energy-loss profile as predicted by SRIM and projected on the vertical axis. The fitting parameters were the length of the vertical component and an overall normalization factor. From both components the angle of the track with respect to the horizontal plane was calculated as well as the total length, which determined the energy of the proton. In this analysis, for each event the actual gas density and the drift velocity were used. An example illustrating the reconstruction procedure is shown in Fig. 4. The uncertainty of the reconstructed energy value is, in principle, different for each event. We found that it is dominated by a systematic uncertainty of the reconstruction procedure itself and that the value of 30 keV is a good measure for the standard deviation for the proton energy below 1 MeV. The principles of the adopted reconstruction procedure are described in more detail in Ref. [23].

A. ^{26}P

Each of the 2463 events corresponding to well implanted ions of ^{26}P was inspected to select decay events. In 477 events
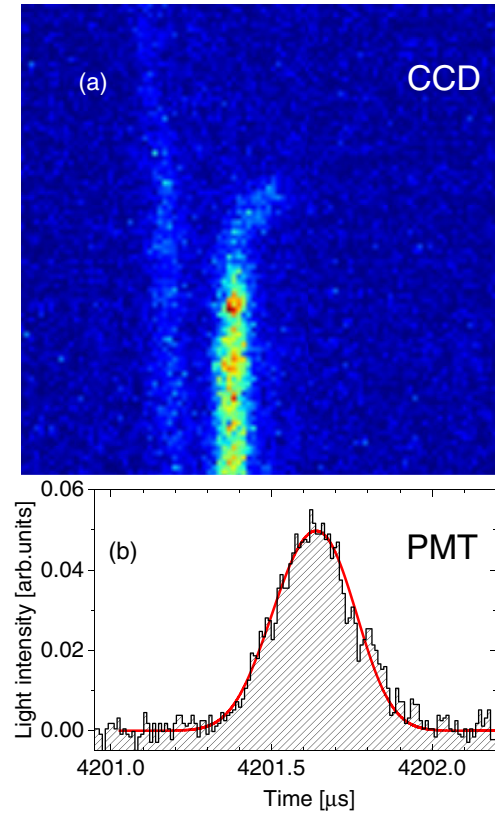

FIG. 4. An example of energy reconstruction of a β-delayed proton emitted after decay of ^{27}S. (a) On the CCD image one sees a track of the ^{27}S ion entering the field of view from below and a shorter and weaker track of the emitted proton. The length of the proton track on the image is 8 mm. The long weaker track on the left represents an ion which passed through the chamber before the triggering ion. (b) A part of the PMT waveform showing the event of proton emission (histogram) which occurred 4.2 ms after the implantation, together with the best fitted SRIM prediction (solid red line). It corresponds to a vertical length of the track of 3 mm. The total length of the track in three dimensions, 8.5 mm, corresponds to a proton energy of 320 keV.

evidence for the decay was observed. In all of them, a clear signal in the PMT waveform was found, providing the timing information. The maximum likelihood analysis yielded a half-life value of $T_{1/2} = 50^{+23}_{-12}$, ms which is consistent with the literature value of 43.7(6) [5]. The large error of our result is caused by the low statistics and the exposure time of 50 ms, which is too short with respect to the measured half-life.

On the CCD images 370 events of βp and 20 events of $\beta 2p$ emission were clearly seen. In the remaining 87 events proton tracks were not visible clearly on the image. We interpret these events as being mostly due to emission of protons of very low energy, in particular those emitted close to the vertical axis, so that their horizontal component is very short. Since there is no reason to doubt that these events represent decays of ^{26}P, we take all 477 events to determine the total branching ratio for both βp and $\beta 2p$ decay channels. Introducing the correction for the finite observation time, we obtain $b_{tot} = 35(2)\%$ which is in agreement within two sigma with the value of 39(2)% published by Thomas *et al.* [5]. In the $\beta 2p$ decays of ^{26}P,
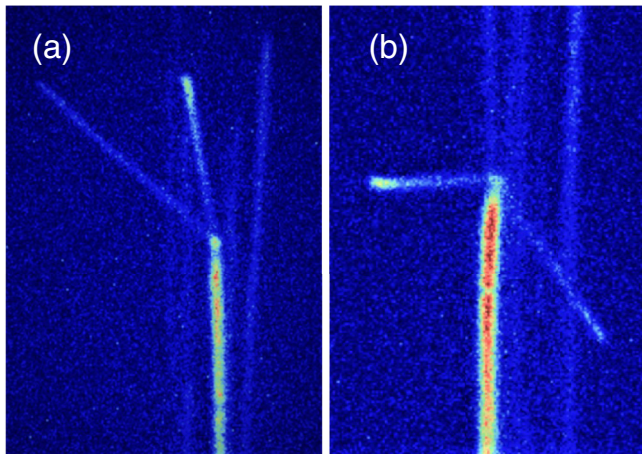
FIG. 5. Example CCD images of $\beta 2p$ decay events following implantation of ^{26}P (a) and ^{27}S (b). The long, weaker tracks represent ions which passed through the chamber before the triggering ion.

FIG. 6. Energy spectrum of β-delayed protons emitted after decay of ^{26}P. The energy is given in the laboratory system.

energy greater than 3.8 MeV is released [5]. Since the two delayed protons share this energy, we assume that all $\beta 2p$ events must be clearly seen on the CCD images and/or on the PMT waveforms. The observed 20 such events yield a branching ratio for the $\beta 2p$ emission of $b_{\beta 2p} = 1.5(4)\%$, again in agreement within two sigma with the value of 2.2(3)% reported in Ref. [5]. It is worth noting that, in contrast to the latter work, our identification of the $\beta 2p$ decay channel in not based on the measurement of proton energies but instead on the clear observation of two proton tracks emitted at the same time by the stopped ion; see Fig. 5. In case one of the protons is emitted vertically and is not seen well on the CCD image, it can still be identified since it leaves a clear, long signal on the PMT waveform. The probability of such an event is, however, very low. The chance that a proton of 2 MeV is emitted into a narrow solid angle around the vertical axis, such that the horizontal projection of its track may be missed on the CCD image, is estimated to be lower than 3×10^{-4}.

In 141 cases of βp emission it was possible to reconstruct the energy of the emitted protons. The resulting spectrum is shown in Fig. 6. The strong peak at low energy corresponds to the transition from the 5.93 MeV state in ^{26}Si to the ground state of ^{25}Al. For the energy of this line we obtain 410(30) keV. By introducing a correction for the recoil, we arrive at a center-of-mass energy of 426(30) keV. This value is consistent with the value of $414.9 \pm 0.6(\text{stat}) \pm 0.3(\text{syst}) \pm 0.6(\text{lit})$ keV, reported previously in the literature [6], although it is less precise. In Fig. 6 we see also events of larger energy, in agreement with the work of Thomas *et al.* [5]. For example the group around 800 keV corresponds to weaker lines of 778 and 866 keV [5].

In the 415 keV line there are 99 counts, which leads to a lower limit for its absolute intensity of 7.4(7)%. We will argue, however, that a better estimate of this value can be obtained by taking into consideration events recorded only by the PMT, which could not be fully reconstructed. According to the SRIM calculation, the range of a 415 keV proton in the OTPC gas mixture, with the range straggling included, is
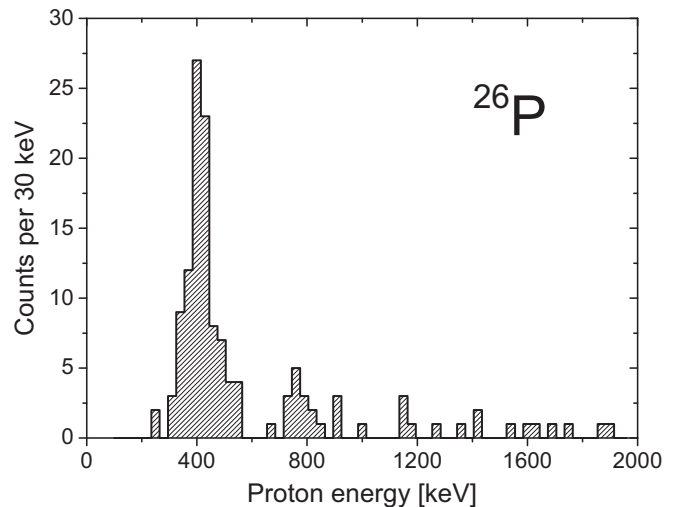
shorter than 13 mm. The next group of events in the spectrum, corresponding to the line at 778 keV [5], starts at about 700 keV. A proton of such energy has a range of at least 25 mm. Its track may have a vertical component shorter than 13 mm but then its horizontal projection would be longer than 20 mm and thus would be clearly visible on the CCD image. Therefore we claim that all events which did not show a clear proton track on the CCD image and have a vertical component shorter than 13 mm belong to the 415 keV line. The analysis of 87 events which were recorded only by the PMT showed that in 41 of them the vertical length could be determined and that in each of them it was in fact shorter than 12 mm. For the remaining 46 events, the vertical length could not be reliably determined. However, some of them may belong to the low energy line in question. Therefore, we conclude that the number of counts in the 415 keV line is larger that 140 and smaller than 186. This leads to an absolute intensity of the 415 keV line in the limits $10.4(9)\% < b_{415} < 13.8(10)\%$. In the Ref. [5] a larger value of 17.96(90)% was determined. In the second peak of the spectrum, which includes 778 and 866 keV lines, we see 15 counts. This yields a branching ratio of 1.1(3)%, while the summed intensity for these two lines given in Ref. [5] is 2.5(3)%.

B. ^{27}S

The same analysis procedure was applied to the case of ^{27}S. All 1237 events with the well implanted ions were inspected individually and in 709 of them decay signals were found, providing good timing information. The maximum likelihood analysis yielded a half-life value of $T_{1/2} = 15.5(16)$ ms, which perfectly coincides with the result reported by Canchel *et al.* [8]. Our decay curve for ^{27}S is presented in Fig. 7.

The CCD images revealed 584 events of βp and 33 events of $\beta 2p$ emission. In the remaining 92 events only the PMT signal was present and no proton tracks could be clearly seen on the image. As in the case of ^{26}P discussed above, we explain these events as mostly coming from delayed protons with a very
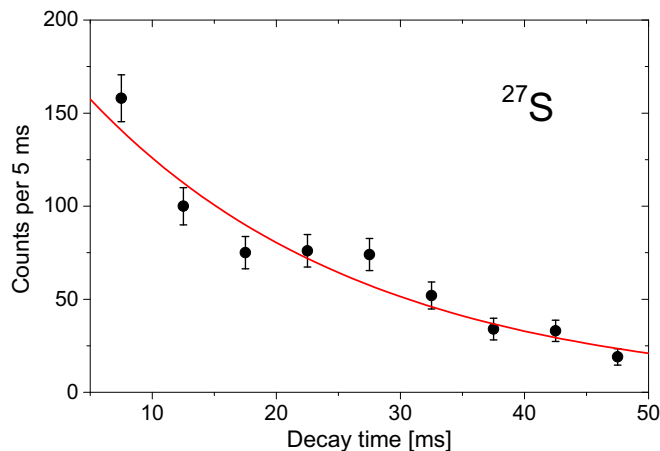
FIG. 7. The measured decay curve of ^{27}S (points). The solid line is the exponential decay curve corresponding to the half-life of ^{27}S.

FIG. 8. Energy spectrum of β-delayed protons emitted after decay of ^{27}S. The energy is given in the laboratory system.

short horizontal component of the track. Therefore, we take all 709 events into account to determine the total branching ratio for βp and $\beta 2p$ decay. With the correction for the finite observation time, we get $b_{tot} = 64(3)\%$, which is larger by an order of magnitude than the value published by Canchel *et al.* [8]. In the $\beta 2p$ decay two protons are expected to share large energy, above 4 MeV according to Ref. [8]. As the case of ^{26}P, we assume that no $\beta 2p$ event occurs without leaving a clear signal on the CCD image. An example of such an event is shown in Fig. 5(b). The recorded 33 $\beta 2p$ events yield a branching ratio for this channel of $b_{\beta 2p} = 3.0(6)\%$ which is larger by a factor of almost 3 than the result of Ref. [8].

Decay of ^{27}S can also be followed by the emission of three delayed protons. Although the sensitivity of the OTPC detector allows one to identify a multiproton emission channel by observation of single event [17–19], we did not observe any $\beta 3p$ decay of ^{27}S. Taking one event as the limiting value, we obtain an upper limit for the relevant branching ratio of $b_{\beta 3p} < 0.1\%$.

The energy reconstruction procedure was successful for 361 βp decay events. The energy spectrum of delayed protons is presented in Fig. 8. Two strong lines appear at the low energy part of the spectrum. They correspond to proton energies in the laboratory system of 320(30) and 710(30) keV. In the center-of-mass system these energies are 332(30) and 737(30) keV, respectively. Evidence for much weaker transitions with higher energies is also present. All βp events shown in Fig. 8 are observed for the first time. We remind the reader that the proton spectrum reported in Ref. [8] starts at 2 MeV.

The two lines at 320 and 710 keV contain 215 counts and 74 counts, respectively. Taking these numbers, we obtain absolute intensities for these lines of 19.6(15)% and 6.7(8)%, respectively. These values have to be considered as lower limits. As in the case of ^{26}P, we argue that more accurate intensity of the 320 keV line can be derived by adding events which did not show a clear proton track on the CCD image and have a vertical component shorter than 10 mm. The events of greater energy have at least 600 keV, so if their vertical component is shorter than 10 mm, the horizontal projection
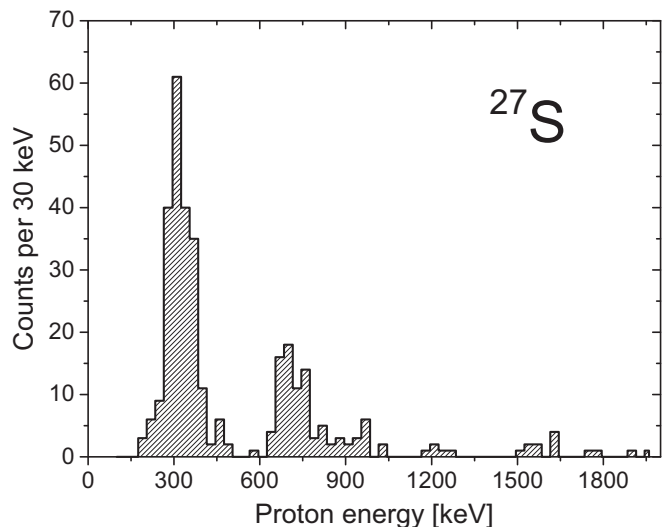
must be at least 17 mm long and thus should be visible on the CCD image. The analysis of 92 events recorded only by the PMT revealed that 52 of them represent a length of the vertical component shorter than 8 mm, while in the remaining 40 the analysis was inconclusive. Thus, the number of counts assigned to the 320 keV line is larger than 267 and smaller than 307. With these limits, the absolute intensity of this line is $24(3)\% < I_{320} < 28(2)\%$.

IV. DISCUSSION

For the case of ^{26}P, our results agree in general with the previous findings for the decay of this nuclide. The total branching for the emission of β-delayed protons, as well as the total branching for the $\beta 2p$ emission determined in our experiment, agree within two sigma with the results of Thomas *et al.* [5]. The energy spectrum of delayed protons, for energy below 2 MeV, is qualitatively consistent with the spectrum from Ref. [5]. Notwithstanding the poor energy resolution of the OTPC detector, the main structures in the spectrum correspond to the lines measured with the telescope of silicon detectors. We note, however, that the spectrum measured by Thomas *et al.* contains a large background, particularly at the low energy end (see Fig. 10 in Ref. [5]), while our spectrum is background free due to insensitivity of the OTPC detector to β electrons. For the absolute intensity of the main structure in the spectrum—a strong line at 415 keV—we find a value smaller by about 30% than the result determined by Thomas *et al.* [5]. The intensity for the two higher-energy lines, not resolved by our detector, is smaller than the summed intensity of these lines given in Ref. [5] by a factor even larger. This factor, however, is less significant due to smaller statistics. Nevertheless, the intensity ratio of the 415 keV line to the sum of the 778 and 866 keV lines, determined from our data, agrees within two sigma with the ratio extracted from the Ref. [5]. This may indicate that the rather complicated absolute normalization procedure in the work of Thomas *et al.*

might have had some uncertainties unaccounted for. In our case, the absolute branching ratios are determined essentially by counting individual events and, except in the case of the low-energy line, where some additional assumptions were made, the procedure is rather straightforward. The comparison of our results for the decay of ^{26}P with those based on measurements conducted with a stack of silicon detectors confirms that the gaseous OTPC detector provides a useful, complementary approach to the study of delayed particle emission.

Among the results obtained for the decay of ^{27}S only, the half-life agrees with the value determined in the previous study by Canchel *et al.* [8]. Both the total absolute branching ratio for delayed emission of protons and the branching for the $\beta 2p$ channel determined by us are much larger than those found in Ref. [8]. The difference in the total branching can be explained by the fact that in the latter work, which used a stack of silicon detectors, only protons of energy greater than about 2 MeV were measured. In contrast, the OTPC detector allowed us to see protons with energies down to about 200 keV. As a result we found that the strongest emission is just below 2 MeV. Concerning the $\beta 2p$ emission, we note that the branching reported for this channel in Ref. [8] results from the identification of two lines in the charged-particle spectrum which were interpreted as the $2p$ emission from the isobaric analog state (IAS) in ^{27}P to the ground state of ^{25}Al. In our experiment we see all $\beta 2p$ events, including those originating from weekly populated states in ^{27}P. We observe and count such events regardless of the β-feeding strength, while the technique applied in Ref. [8] requires peaks to be observed in the spectrum on top of the background. Our result for the $\beta 2p$ branching suggests that, in addition to the IAS, other $2p$-emitting states in ^{27}P are fed in the decay of ^{27}S. Again, the key advantage of the OTPC detector is the absence of background due to β particles and the counting of individual, identified events. However, a drawback of our method is that high-energy protons do not stop within the active volume and we cannot reconstruct their energy.

In the βp spectrum of ^{27}S two lines are clearly observed, corresponding to center-of-mass decay energies of 332(30) and 737(30) keV. We interpret them as representing transitions from the $3/2^+$ and $5/2^+$ levels in ^{27}P, respectively, to the ground state of ^{26}Si. We proceed to see how the energies of these lines affect the decay scheme of ^{27}S. We start from the mass of ^{26}Si, which among the relevant nuclei is known with the highest precision. Its mass excess was measured to be $-7141.0(1)$ keV [24]. Further, we assume that the excitation energy of the $3/2^+$ state in ^{27}P is equal to 1120(8) keV, as given by γ spectroscopy [13], which is more precise than values obtained by kinematical reconstruction of measured particles [9–11]. With these assumptions the proton transition energy of 332(30) keV yields a proton separation energy for ^{27}P of 788(30) keV and a mass excess of its ground state equal to $-640(30)$ keV. This value is larger than the value of $-722(26)$ keV given by the NUBASE2012 evaluation [24]. However, due to large uncertainties, both values are consistent within the three sigma value. From the energy difference of the two proton transitions the excitation energy of the $5/2^+$ state in ^{27}P comes out as 1525(43) keV. This value is smaller than
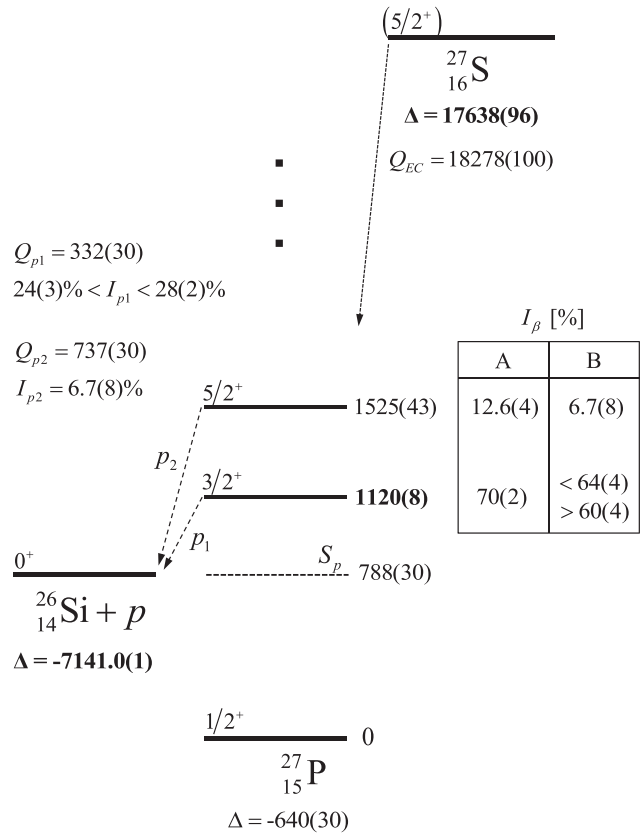
FIG. 9. Part of the decay scheme of ^{27}S showing levels discussed in this work. Energy values are given in keV. The values taken from literature are written in bold. In the table the β feeding probabilities are given calculated in two approximations: (A) from the measured $\log ft$ values in the decay of ^{27}Na assuming exact mirror symmetry, and (B) assuming that only the first excited $3/2^+$ state has a non-negligible γ decay branch. The drawing is not to scale. See text for more details and for references.

results of Refs. [9,10] but it is in a reasonable agreement with the value of 1592(62) keV, recently reported by Marganiec *et al.* [11]. The resulting scheme of the levels discussed is shown in Fig. 9.

Next, we investigate the γ-to-proton emission probability ratio, Γ_γ / Γ_p, which is important in the description of the ^{26}Si$(p,\gamma)^{27}$P reaction rate. First, we use the mirror symmetry and assume that the $\log ft$ values for the corresponding transitions are the same as those measured in the decay of ^{27}Na [12]. With the mass excess of ^{27}S determined by Canchel *et al.* [8] and our result for ^{27}P, the decay energy of ^{27}S is $Q_{EC} = 18.28(10)$ MeV. Combining all relevant data we arrive at absolute intensities of the direct β feeding of 70(2)% and 12.6(4)% for the $3/2^+$ and $5/2^+$ states of ^{27}P, respectively; see Fig. 9. These levels can deexcite only by emission of a proton to the ground state of ^{26}Si or by γ radiation. The β feeding of the $5/2^+$ state, together with the absolute intensity of the proton transition from this state of about 7%, suggest that the proton width of the $5/2^+$ state is of the same order as its γ width. This is very unlikely. According to all models discussed in the literature the proton width Γ_p of this state is expected to

be from four to five orders of magnitude larger than the γ width Γ_γ [9,11,25]. For a plausible explanation of this discrepancy, we note that the log ft data in the decay of ^{27}Na, evaluated in Ref. [12], come from a γ spectroscopy measurement which used a detector setup of rather lowefficiency [26] and thus was not sensitive to high energy transitions deexciting high-energy levels in ^{27}Mg. It is probable that this study suffered from the Pandemonium effect [27]. Consequently the determined β feedings are overestimated and the log ft values underestimated.

In the second approach we adopt the assumption that, except for the first $3/2^+$ state, all other excited states of ^{27}P decay only by proton emission. Then the branching ratio for the γ decay of the first $3/2^+$ level is equal to $1 - b_{tot} = 0.36(3)$, where b_{tot} is the total branching ratio for the emission of delayed protons in the decay of ^{27}S; see Sec. III B. Then our two limits for the proton emission probability from the $3/2^+$ state lead to β feeding of this state in the range from 60(4)% to 64(4)% and to a value of Γ_γ / Γ_p in the range from 1.3(2) to 1.5(2). The most recent model calculation, made by Marganiec *et al.* [11] to determine the resonance strength in the radiative proton capture by ^{26}Si, yielded a value of 1.82 for this ratio, while the previous calculations predicted smaller values ranging from 0.32 [10] through 0.8 [25] to 0.98 [9]. Our result is located between the latter value and that of Ref. [11].

V. SUMMARY AND OUTLOOK

We have studied β decay of ^{26}P and ^{27}S with the focus on the emission of delayed protons. The ions of interest, produced in the fragmentation reaction of a ^{32}S beam, selected and identified in flight with the ACCULINNA separator, were implanted into the active volume of the gaseous OTPC detector where the tracks of delayed protons were recorded. This allowed for the determination of the total branching ratio for the βp and $\beta 2p$ decay channels. The tracks of protons with energy below 2 MeV could be reconstructed, providing the low energy spectra of β-delayed protons. The results obtained for the decay of ^{26}P were found to be consistent with the previous study of Thomas *et al.* [5]. In contrast, the total branching ratio for the emission of delayed protons by ^{27}S was found to be an order of magnitude larger than results of the previous measurement by Canchel *et al.* [8]. A part of this discrepancy

is due to low-energy part of the proton spectrum, which could not be accessed before [8]. In particular, we observe two strong proton lines representing transitions from the first two excited states of ^{27}P to the ground state of ^{26}Si. By assuming that only the first excited $3/2^+$ state of ^{27}P has the γ deexcitation branch, while the all higher-lying states decay only by proton emission, we determined the γ-to-proton probability ratio Γ_γ / Γ_p for this $3/2^+$ state to be in the range from 1.3(2) to 1.5(2).

An attempt to exploit the mirror symmetry to estimate the log ft values for the decay of ^{27}S suggests that the log ft measured for the decay of its mirror partner ^{27}Na [12,26] are underestimated. More precise spectroscopic studies of both nuclei are needed to clarify a possible mirror asymmetry. Such studies would be particularly interesting in view of the reported asymmetry in the decays of ^{26}P and ^{26}Na [7].

In this work we have shown that the key parameters for the resonant part of the ^{26}Si$(p,\gamma)^{27}$P reaction rate can be determined by the β-delayed proton spectroscopy of ^{27}S in a rather straightforward way. The technique based on a time projection chamber, employed here, is preferred for the clean identification of decay channels and for the precise determination of their absolute branching ratios. The exact energies of the relevant resonances and the probability ratios of γ-to-proton emission can be established accurately using a compact telescope of silicon detectors surrounded by an array of germanium detectors. Thus the most advantageous approach would combine results provided by both complementary techniques.

[1] B. Blank and M. J. G. Borge, Prog. Part. Nucl. Phys. **60**, 403 (2008).

[2] M. Pfützner, M. Karny, L. V. Grigorenko, and K. Riisager, Rev. Mod. Phys. **84**, 567 (2012).

[3] N. Prantzos and R. Diehl, Phys. Rep. **267**, 1 (1996).

[4] C. Iliadis, L. Buchmann, P. M. Endt, H. Herndl, and M. Wiescher, Phys. Rev. C **53**, 475 (1995).

[5] J.-C. Thomas *et al.*, Eur. Phys. J. A **21**, 419 (2004).

[6] M. B. Bennett *et al.*, Phys. Rev. Lett. **111**, 232503 (2013).

[7] D. Pérez-Loureiro *et al.*, Phys. Rev. C **93**, 064320 (2016).

[8] G. Canchel *et al.*, Eur. Phys. J. A **12**, 377 (2001).

[9] J. A. Caggiano *et al.*, Phys. Rev. C **64**, 025802 (2001).

[10] Y. Togano *et al.*, Phys. Rev. C **84**, 035808 (2011).

[11] J. Marganiec *et al.*, Phys. Rev. C **93**, 045811 (2016).

[12] M. S. Basunia, Nucl. Data Sheets **112**, 1875 (2011).

[13] A. Gade *et al.*, Phys. Rev. C **77**, 044306 (2008).

[14] K. Miernik *et al.*, Nucl. Instrum. Methods Phys. Res., Sect. A **581**, 194 (2007).

[15] K. Miernik *et al.*, Phys. Rev. Lett. **99**, 192501 (2007).

[16] M. Pomorski *et al.*, Phys. Rev. C **90**, 014311 (2014).

[17] K. Miernik *et al.*, Phys. Rev. C **76**, 041304(R) (2007).

[18] M. Pomorski *et al.*, Phys. Rev. C **83**, 014306 (2011).

[19] A. A. Lis *et al.*, Phys. Rev. C **91**, 064309 (2015).

[20] A. M. Rodin *et al.*, Nucl. Instrum. Methods B **126**, 236 (1996).

[21] F. Sauli, Nucl. Instrum. Methods Phys. Res., Sect. A **580**, 971 (2007).

[22] J. F. Ziegler, The Stopping and Range of Ions in Matter (SRIM), http://www.srim.org; accessed on 25 February 2016.

[23] M. Pfützner *et al.*, Phys. Rev. C **92**, 014316 (2015).

[24] G. Audi *et al.*, Chinese Phys. C **36**, 1157 (2012).

[25] H. Herndl, J. Görres, M. Wiescher, B. A. Brown, and L. Van Wormer, Phys. Rev. C **52**, 1078 (1995).

[26] D. Guillemaud-Mueller *et al.*, Nucl. Phys. A **426**, 37 (1984).

[27] J. C. Hardy *et al.*, Phys. Lett. B **71**, 307 (1977).